THEORETICA CHIMICA ACTA

Theoret. Chim. Acta (Berl.) 62, 39–53 (1982)

Diatomic Interactions in Momentum Space. The Effect of Polarization and Floating Functions

Toshikatsu Koga, Kenji Shimokawa, Ikuo Inagawa, and Mutsuo Morita

Department of Applied Chemistry and Department of Applied Science for Energy, Muroran Institute of Technology, Muroran, Hokkaido, 050 Japan

The method of momentum density for interatomic interactions is used to investigate the pictures and roles of the polarization and floating functions in momentum (p-) space. Referring to the previous results from the minimal LCAO (Finkelstein–Horowitz) momentum density, we quantitatively discuss the effect of these functions for the bonding process in the ground state of H_2^+ system. The essence of the polarization and floating effects is found to be a modulation of the oscillation in the two-center part of the momentum density. The polarization function introduces a term with a phase and the floating function enlarges the period of the oscillation. An increased migration of the density from the one-center to the two-center part is also important. As a result, both the functions contribute to emphasize the contraction and expansion of momentum density observed previously. However, the floating function disturbs the density distribution in high momentum region, reflecting the destruction of cusps in position (r-) space. We point out an error in the pioneer work of Duncanson.

Key words: Momentum density – Polarization function – Floating function.

1. Introduction

Recently [1–5], we have proposed and developed a method of momentum density which enables us to understand the origin of various nuclear rearrangement processes of molecular systems from the momentum (p-) space point of view. Based on the virial theorem, we have derived three sets of fundamental equations of this approach which rigorously relate the momentum density to the energy

0040-5744/82/0062/0039/$03.00

E and interatomic force F of a system [1]. These equations have been used to investigate the reorganization of the momentum density and its energetic contribution during interaction processes. We have then suggested that the contraction and expansion of momentum density are important concepts which characterize the nature of interactions in p-space.

The momentum density approach has been applied to the attractive $1s\sigma_g$ and repulsive $2p\sigma_u$ states of H_2^+ system [2]. Based on the Finkelstein–Horowitz (FH) wave function [6], the predicted density reorganizations of the contraction and expansion have been shown to actually occur. The contributions of these density behaviours to the stabilization and destabilization of the system have been examined quantitatively together with their atom–bond and parallel–perpendicular partitionings. The method has been also applied to the $2p\pi_u$ and $3d\pi_g$ states of the same system and the concept of this approach has been shown to be valid and common to both the σ and π states [4]. We have further shown that rigorous relations between the energy and the momentum density can be deduced from the integrated Hellmann–Feynman theorem [7] with respect to the electron mass [3]. More recently, the approach has been proved to be applicable to a wide range of nuclear rearrangement problems, in which several bond lengths or bond angles may be concerned in a complicated manner [5].

The purpose of this paper is to study the pictures and roles of the polarization (for example, see [8–10]) and floating [10–12] functions from the p-space point of view. Because of the increased variational freedom, both the polarization and floating functions certainly improve the density distribution with a concomitant decrease in the energy. A position (r-) space picture of this improvement can be obtained from the electrostatic Hellmann–Feynman theorem [13, 14] which connects the position density with the quantum-mechanical force exerting on nucleus: During the bonding process, the in-phase mixing and inward floating of the respective functions accelerate the polarization of atomic density and the accumulation of bond density, which result in an increase of the driving force of the bond formation. The increase in attractive force is a direct reflection of the decrease in energy caused by the polarization and floating effects appearing in the position density (cf. integrated Hellmann–Feynman theorem [7]).

In the following, we investigate the corresponding pictures and roles of the polarization and floating functions in p-space by using the proposed method of momentum density [1–5]. We have again chosen the $1s\sigma_g$ state of H_2^+ system which is a prototype of the covalent bonding, and for which the results of the minimal LCAO momentum density have been already known [2]. The present method of momentum density is outlined in the next section. The polarization and floating effects are qualitatively discussed in Sect. 3 based on the p-representation of the functions. In Sect. 4, we quantitatively examine the effects of the polarization and floating functions on the momentum density during the bonding process.

We use atomic units throughout this paper.

2. Basic Concepts of Momentum Density Approach

In the momentum density approach, either of $\rho(\mathbf{p})$, $I(p)$, or $J(q)$ is acceptable as the basic physical quantity [5], where $\rho(\mathbf{p})$ is the three-dimensional momentum density, $I(p)$ $[\equiv \int_0^{2\pi} d\phi_p \int_0^{\pi} d\theta_p p^2 \sin\theta_p \rho(\mathbf{p})]$ the radial momentum density, and $J(q)[\equiv (1/2)\int_{|q|}^{\infty} dp\, p^{-1} I(p)]$ the Compton profile. The same guiding principles hold for the behaviours of these quantities. For simplicity, we here proceed with our study using the radial density and Compton profile.

The basic equations, which exactly relate the momentum density to the kinetic energy ΔT, the stabilization energy ΔE, and the interatomic force F of a diatomic system, are given by [1, 2]

$$\Delta T(R) \equiv T(R) - T(\infty) = \int_0^{\infty} dp\ (p^2/2)\Delta I(p; R), \tag{1a}$$

$$\Delta E(R) \equiv E(R) - E(\infty) = \int_0^{\infty} dp\ (p^2/2)\Delta \bar{I}(p; R), \tag{1b}$$

$$F(R) \equiv -dE(R)/dR = (1/R)\int_0^{\infty} dp\ (p^2/2)\Delta \tilde{I}(p; R), \tag{1c}$$

where $p = |\mathbf{p}|$, R the internuclear distance, and the reorganizations in the radial momentum density are defined by

$$\Delta I(p; R) \equiv I(p; R) - I(p; \infty), \tag{2a}$$

$$\Delta \bar{I}(p; R) \equiv (1/R)\int_R^{\infty} dR'\, \Delta I(p; R'), \tag{2b}$$

$$\Delta \tilde{I}(p; R) \equiv \Delta I(p; R) + \Delta \bar{I}(p; R). \tag{2c}$$

Eq. (1) holds for all $I(p)$ as far as their parent wave functions satisfy the virial theorem. Because of the conservation of the number of electrons, the density differences ΔI, $\Delta \bar{I}$, and $\Delta \tilde{I}$ vanish identically when integrated over all p range. Then from Eq. (1), we can deduce the guiding principles of contraction and expansion which govern the nature of interactions [1]. (Contraction means an increase of low momentum density with a simultaneous decrease of high momentum density, while expansion means the opposite redistribution.) For example, the contraction/expansion of ΔI imply $\Delta T < 0 / \Delta T > 0$ respectively and are important for the initiation/termination of chemical reactions. The contraction/expansion of $\Delta \bar{I}$ result in $\Delta E < 0$ (stabilization)/$\Delta E > 0$ (destabilization) and the degree of contraction is largest at equilibrium distance. The contraction/expansion of $\Delta \tilde{I}$ correspond to $F < 0$ (attraction)/$F > 0$ (repulsion) and their critical point may be identical with the equilibrium point ($F = 0$).

Two energy partitionings are examined here based on Eqs. (1) and (2). One is atom–bond partitioning which results from the separation of $I(p)$ into one-center (atom) and two-center (bond) parts;

$$\Delta E(R) = \Delta E_{\text{atom}}(R) + \Delta E_{\text{bond}}(R), \tag{3a}$$

$$\begin{cases} \Delta E_{\text{atom}}(R) = \int_0^\infty dp\ (p^2/2)\,\Delta\bar{I}_{\text{atom}}(p;R), & \text{(3b)} \\ \Delta E_{\text{bond}}(R) = \int_0^\infty dp\ (p^2/2)\,\Delta\bar{I}_{\text{bond}}(p;R). & \text{(3c)} \end{cases}$$

The other is parallel ($\parallel$) – perpendicular ($\perp$) partitioning which results from the separation of the kinetic operator into the three directional components along and normal to the bond axis;

$$\Delta E(R) = \Delta E_{\parallel}(R) + 2\Delta E_{\perp}(R), \tag{4a}$$

$$\begin{cases} \Delta E_{\parallel}(R) = \int_{-\infty}^{+\infty} dp_{\parallel}\ (p_{\parallel}^2/2)\Delta\bar{J}_{\parallel}(p_{\parallel};R), & \text{(4b)} \\ \Delta E_{\perp}(R) = \int_{-\infty}^{+\infty} dp_{\perp}\ (p_{\perp}^2/2)\Delta\bar{J}_{\perp}(p_{\perp};R), & \text{(4c)} \end{cases}$$

where $\Delta\bar{J}_{\parallel}$ and $\Delta\bar{J}_{\perp}$ are obtained from Eq. (2) by replacing $I(p)$ with the directional Compton profiles $J_{\parallel}(p_{\parallel}) = \int_{-\infty}^{+\infty} dp_{\perp} \int_{-\infty}^{+\infty} dp_{\perp'}\,\rho(\mathbf{p})$ and $J_{\perp}(p_{\perp}) = \int_{-\infty}^{+\infty} dp_{\parallel} \int_{-\infty}^{+\infty} dp_{\perp'}\,\rho(\mathbf{p})$. We can partition ΔT and F in the same way.

3. Polarization and Floating Functions in Momentum Space

3.1. Polarization Function

The wave function for the $1s\sigma_g$ state of H_2^+, which consists of the $1s$ AOs and the additional $2p\sigma$ polarization AOs, has been referred to as Dickinson (DK) function [15], and is given by

$$\Psi(\mathbf{r}) = (2+2S)^{-1/2}\{\chi_A(\mathbf{r}) + \chi_B(\mathbf{r})\}, \tag{5a}$$

$$\begin{cases} \chi_A(\mathbf{r}) = c_1 1s_A(\mathbf{r}) + c_2 2p\sigma_A(\mathbf{r}). & \text{(5b)} \\ \chi_B(\mathbf{r}) = c_1 1s_B(\mathbf{r}) - c_2 2p\sigma_B(\mathbf{r}), & \text{(5c)} \\ 1s_A(\mathbf{r}) = (\zeta^3/\pi)^{1/2} \exp(-\zeta|\mathbf{r}-\mathbf{R}_A|), & \text{(5d)} \\ 2p\sigma_A(\mathbf{r}) = (\zeta^5/\pi)^{1/2}|\mathbf{r}-\mathbf{R}_A|\cos\theta_A \exp(-\zeta|\mathbf{r}-\mathbf{R}_A|), & \text{(5e)} \end{cases}$$

where S is the overlap integral, $\mathbf{R}_A$ the position vector of nucleus A ($R = |\mathbf{R}_B - \mathbf{R}_A|$) and θ_A the angle between the vectors $\mathbf{r}-\mathbf{R}_A$ and $\mathbf{R}_B-\mathbf{R}_A$. The exponent ζ and the coefficients c_1 and c_2 are variationally optimized for every R, and this guarantees the validity of Eq. (1).

The Dirac–Fourier transformation [16] of Eq. (5) yields the corresponding p-space wave function

$$\psi(\mathbf{p}) = (2+2S)^{-1/2}\{\chi_A(\mathbf{p}) + \chi_B(\mathbf{p})\}, \tag{6a}$$

$$\begin{cases} \chi_A(\mathbf{p}) = \exp(-i\mathbf{p}\mathbf{R}_A)\{c_1 1s(\mathbf{p}) + c_2 2p\sigma(\mathbf{p})\}, & \text{(6b)} \\ \chi_B(\mathbf{p}) = \exp(-i\mathbf{p}\mathbf{R}_B)\{c_1 1s(\mathbf{p}) - c_2 2p\sigma(\mathbf{p})\}, & \text{(6c)} \end{cases}$$

$$\begin{cases} 1s(\mathbf{p}) = 2^{3/2}\pi^{-1}\zeta^{5/2}(p^2+\zeta^2)^{-2}, & (6d) \\ 2p\sigma(\mathbf{p}) = -i2^{7/2}\pi^{-1}\zeta^{7/2}p(p^2+\zeta^2)^{-3}\cos\theta_p, & (6e) \end{cases}$$

where the spherical polar coordinates $\mathbf{p} = (p, \theta_p, \phi_p)$ are used with the p_z axis parallel to the bond axis. Then the radial density is found to be

$$I(p;R) = I_{\text{atom}}(p;R) + I_{\text{bond}}(p;R), \tag{7a}$$

$$\begin{cases} I_{\text{atom}}(p;R) = 2^5\pi^{-1}\zeta^5(1+S)^{-1}p^2\{c_1^2(p^2+\zeta^2)^{-4} \\ \qquad + c_2^2 2^4 3^{-1}\zeta^2 p^2(p^2+\zeta^2)^{-6}\}, & (7b) \\ I_{\text{bond}}(p;R) = 2^5\pi^{-1}\zeta^5(1+S)^{-1}p^2\{c_1^2(p^2+\zeta^2)^{-4}(Rp)^{-1}\sin(Rp) \\ \qquad + c_1c_2 2^3 R^{-1}\zeta(p^2+\zeta^2)^{-5}[(Rp)^{-1}\sin(Rp) - \cos(Rp)] \\ \qquad + c_2^2 2^4 R^{-1}\zeta^2(p^2+\zeta^2)^{-6}[2R^{-2}p^{-1}\sin(Rp) \\ \qquad - 2R^{-1}\cos(Rp) - p\sin(Rp)]\}, & (7c) \end{cases}$$

and the directional Compton profiles are

$$\begin{aligned} J_{\parallel}(p_{\parallel};R) = {} & 2^3\pi^{-1}\zeta^5(1+S)^{-1}\{c_1^2 3^{-1}(p_{\parallel}^2+\zeta^2)^{-3}[1+\cos(Rp_{\parallel})] \\ & + c_1c_2 2\zeta p_{\parallel}(p_{\parallel}^2+\zeta^2)^{-4}\sin(Rp_{\parallel}) \\ & + c_2^2 2^4 5^{-1}\zeta^2 p_{\parallel}^2(p_{\parallel}^2+\zeta^2)^{-5}[1-\cos(Rp_{\parallel})]\}, \end{aligned} \tag{8a}$$

$$\begin{aligned} J_{\perp}(p_{\perp};R) = {} & \pi^{-1}\zeta^5(1+S)^{-1}\{c_1^2 3^{-1}[2^3(p_{\perp}^2+\zeta^2)^{-3} + R^3(p_{\perp}^2+\zeta^2)^{-3/2}K_3(z)] \\ & + c_1c_2 3^{-1}\zeta R^4(p_{\perp}^2+\zeta^2)^{-3/2}K_3(z) \\ & + c_2^2 5^{-1}\zeta^2[2^4(p_{\perp}^2+\zeta^2)^{-4} \\ & - R^4 3^{-1}(p_{\perp}^2+\zeta^2)^{-2}(K_4(z) - zK_3(z))]\}, \end{aligned} \tag{8b}$$

where $z = R(p_{\perp}^2+\zeta^2)^{1/2}$ and $K_{\nu}(z)$ the modified Bessel function of order ν [17]. The reorganizations from the isolated atoms are obtained by subtracting the corresponding quantities for the hydrogen atom, $I_{\text{atom}}(p;\infty) = 2^5\pi^{-1}p^2(p^2+1)^{-4}$, $I_{\text{bond}}(p;\infty) = 0$, $J_{\parallel}(p_{\parallel};\infty) = 2^3 3^{-1}\pi^{-1}(p_{\parallel}^2+1)^{-3}$, and $J_{\perp}(p_{\perp};\infty) = J_{\parallel}(p_{\perp};\infty)$.

If we set $c_1 = 1$ and $c_2 = 0$ and optimize only ζ, the above results (5–8) reduce to those for the Finkelstein–Horowitz (FH) wave function [6], which were examined previously [2] and are the reference in the present study of polarization and floating effects.

Now we discuss the polarization effect in p-space based on the functional forms of the radial densities and Compton profiles. As a first approximation of the effect, we examine the part proportional to c_1c_2 which arises from the interaction between the $1s$ on one nucleus and the $2p\sigma$ on the other, since the coefficient c_2 is at most a sixth of c_1 during the bonding process. (Note that the c_1c_2 part also appears in the overlap integral S and S_{DK} is larger than S_{FH}.) The atom part (Eq. (7b)) does not contain the c_1c_2 term, and is same in form as FH, i.e., a monotonic function $p^2(p^2+\zeta^2)^{-4}$ with a peak at $p = 3^{-1/2}\zeta$. However, since $S_{\text{DK}} > S_{\text{FH}}$ and $c_1^2 < 1$, the polarization effect reduces the scale of the distribution

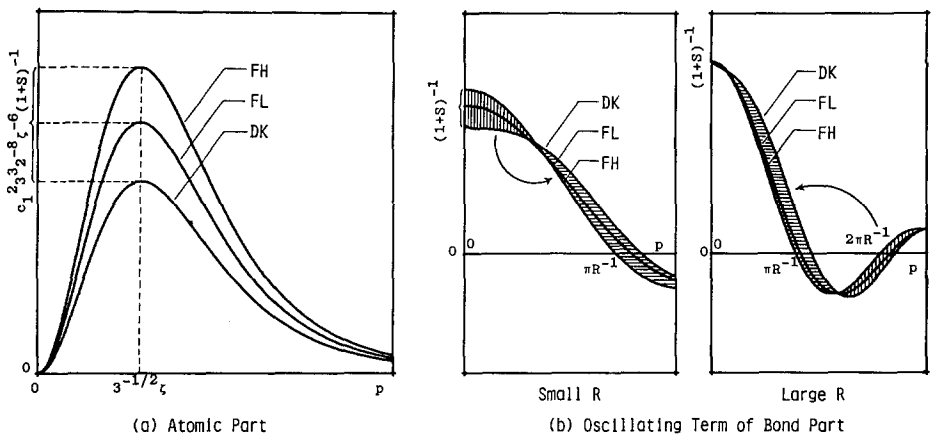

Fig. 1. Schematic representation of the polarization and floating effects on the atom and bond parts of the radial momentum density

and decreases the atomic charge (Fig. 1a). On the other hand, the c_1c_2 term in the bond part (Eq. (7c)) is an oscillating function $(Rp)^{-1}\sin(Rp)-\cos(Rp)$ with the "envelope" function $2^8\pi^{-1}R^{-1}\zeta^6(1+S)^{-1}p^2(p^2+\zeta^2)^{-5}$. This trigonometric part can be rewritten as $[1+(Rp)^{-2}]^{1/2}\sin[Rp-\arctan(Rp)]$ and includes a "phase" arctan (Rp) which takes a value between 0 and $\pi/2$. In the DK density, the oscillation of the bond part is modulated by the mixing of the corrective c_1c_2 term into the FH part with $(Rp)^{-1}\sin(Rp)$ so as to shift towards higher p region. Then for a large R where $S_{DK}\sim S_{FH}$, the DK bond density migrates into lower p region than the FH density due to this modulation (see the right of Fig. 1b). For a small R where $S_{DK}>S_{FH}$, however, the DK density inversely migrates into higher p region, since the "envelope" of DK becomes smaller than that of FH (see the left of Fig. 1b). Consequently, the polarization effect contributes to increase the low momentum density at a large R and to increase the high momentum density at a small R, through the modulation of the bond part and the increased density transfer from the atom to the bond part.

For the parallel part (Eq. (8a)) of the directional partitioning, the correction term of $\sin(Rp_\parallel)$ is added which differs from the FH term of $\cos(Rp_\parallel)$ by the phase $\pi/2$. Therefore, the polarization effect on this part is expected to be similar to that on the bond part. The correction term for the perpendicular part (Eq. (8b)) has the same functional form as the parent FH density $((p_\perp^2+\zeta^2)^{-3/2}K_3(R[p_\perp^2+\zeta^2]^{1/2}))$ and no essential difference is observed.

The distributions $I(p)$ and $J_\parallel(p_\parallel)$ of the $2p\sigma$ AO are more expansive and $J_\perp(p_\perp)$ is more contractive than those of the $1s$ AO. When the terms proportional to c_2^2 are taken into account, these characters may be introduced as the second-order correction to the FH distributions.

In the derivation of the DK momentum density (Eq. (7)), we have found a significant error in the pioneer work of Duncanson [18]. In his expression for the momentum density, the c_1c_2 term is dropped out (Eq. (6) of Ref. [18]) and

he concluded that there is little difference between the DK and FH densities (Fig. 1 of Ref. [18]). (The error seems to have been caused by the confusion of the left- and right-handed coordinate systems for the $2p\sigma$ AOs in transforming the wave function from r- to p-space.) However, as discussed above, the c_1c_2 terms are shown to play an important role of the polarization effect in the improvement of the momentum density and Compton profile (see Sect. 4 for quantitative discussion).

3.2. Floating Function

Setting $c_1 = 1$ and $c_2 = 0$ and substituting $R' = R - 2x$ for R in Eqs. (5–8), we obtain expressions for the floating (FL) function, where x stands for the displacement of the center of the $1s$ AO from the nucleus and is taken to be positive when the AO floats inside the bond. The FL function is a generalization of the FH function by the introduction of another variational parameter x and the simultaneous optimization of x and ζ.

The floating effect on the atom part of the momentum density merely reduces the scale of the distribution, since the inward floating ($x > 0$) results in $S_{\mathrm{FL}} > S_{\mathrm{FH}}$ (Fig. 1a). The oscillation of the bond part depends on $(R'p)^{-1} \sin(R'p)$, and is modulated by the positive x so as to increase its period than that of FH. Then for a large R where $S_{\mathrm{FL}} \sim S_{\mathrm{FH}}$, the floating effect transfers the bond density towards the low p region, whereas for a small R where $S_{\mathrm{FL}} > S_{\mathrm{FH}}$ and the envelope is smaller, it causes a reverse migration of the bond density (Fig. 1b). The results are parallel to those of the polarization effect. This parallelism is also supported by the fact that the Taylor expansion of the FL oscillation is $(Rp)^{-1} \sin(Rp) + \{2R^{-1}[(Rp)^{-1} \sin(Rp) - \cos(Rp)]\}x + O(x^2)$ and its first-order term is identical with the c_1c_2 part of the DK oscillation. In the directional Compton profiles, the parallel part suffers the effect similar to that on the bond part, since it is in proportion to $\cos(R'p_{\parallel})$ with a longer period than FH. The perpendicular part contains $R'^3K_3(R'[p_\perp^2 + \zeta^2]^{1/2}) = R^3K_3(R[p_\perp^2 + \zeta^2]^{1/2}) + \{2[p_\perp^2 + \zeta^2]^{1/2}R^3K_2(R[p_\perp^2 + \zeta^2]^{1/2})\}x + O(x^2)$ and hence little change is expected since the first-order term behaves similarly to the zeroth-order FH term.

3.3 Discussion

From the above analysis, the essence of the polarization and floating effects is clarified to be the modulation of the oscillation in the two-center part of momentum density. Both the effects lead to an increase of the low momentum density for a large R and to an increase of the high momentum density for a small R. According to our previous study [2], the reorganization of the FH density from the separated atoms is contraction for $R > 2.7$ and expansion for $R < 2.7$. Then the polarization and floating effects contribute to increase the contraction and expansion of the momentum density for the respective R ranges.

The primary pictures of the polarization and floating functions in r-space are the inward polarization of atomic density and the increased density accumulation

in the bond region [10]. However, the corresponding picture in p-space is distinguished between the contraction at a large R and the expansion at a small R. This implies that we must understand the increase of the position density in the internuclear region as the density delocalization at a large R, while as the density localization at a small R.

It is clear from the virial theorem and the equation derived from it that these increases in the contraction and expansion result in a stabilization of the system [1]. For a large R, a decrease in ΔT due to the increased contraction lowers ΔE

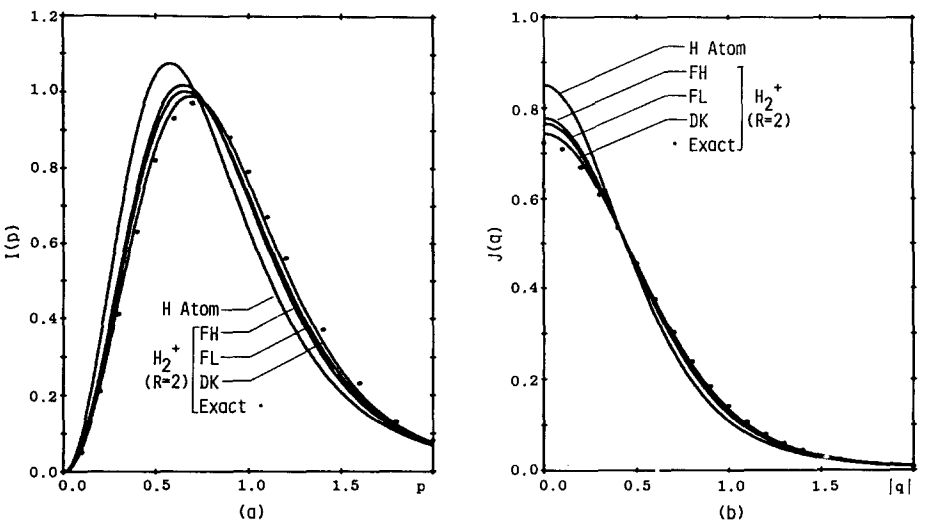

Fig. 2. Radial momentum densities $I(p)$ and isotropic Compton profiles $J(q)$ calculated from the FH, FL, DK, and exact functions for the $1s\sigma_g$ state of H_2^+ molecule

Table 1. First three nodal points on the p_z axis calculated from several wave functions for the ground state of H_2^+ molecule ($R = 2$)[a]

Wave function	D_e	Nodal points		
		1st	2nd	3rd
Finkelstein–Horowitz	0.08651	1.571	4.712	7.854
Floating	0.09416	1.732	5.197	8.662
Dickinson[b]	0.09980	1.860	4.866	7.953
Dickinson[c]	0.10036	1.886	4.932	8.003
Exact[d]	0.10263	2.03	4.98	8.07

[a] Because of the inversion-symmetry of the p-space wave function, the nodes for $p_z > 0$ are given.
[b] With the same exponent for the $1s$ and $2p\sigma$ AOs.
[c] With the separately-optimized exponents for the $1s$ and $2p\sigma$ AOs.
[d] Nodal points are taken from Ref. [21] and D_e from Ref. [22].

through the relation $\Delta E(R) = (1/R)\int_R^\infty dR'\,\Delta T(R')$. In the vicinity of the equilibrium distance R_e, an increase in ΔT due to the increased expansion again lowers ΔE through the relation $\Delta E \sim -\Delta T$. These reorganizations of the momentum electron density and the resultant effects on the stabilization energy are more directly connected by the use of the modified density difference $\Delta\bar{I}(p;R)$ which was introduced previously [1, 2] and is quantitatively examined in the next section.

4. Polarization and Floating Effects during the Bonding Process

In Fig. 2, the radial momentum densities $I(p)$ and the isotropic Compton profiles $J(q)$ obtained from the DK, FL, and FH functions are shown for the equilibrium H_2^+ molecule ($R = 2$) and compared with the exact [19, 20] and hydrogen-atomic

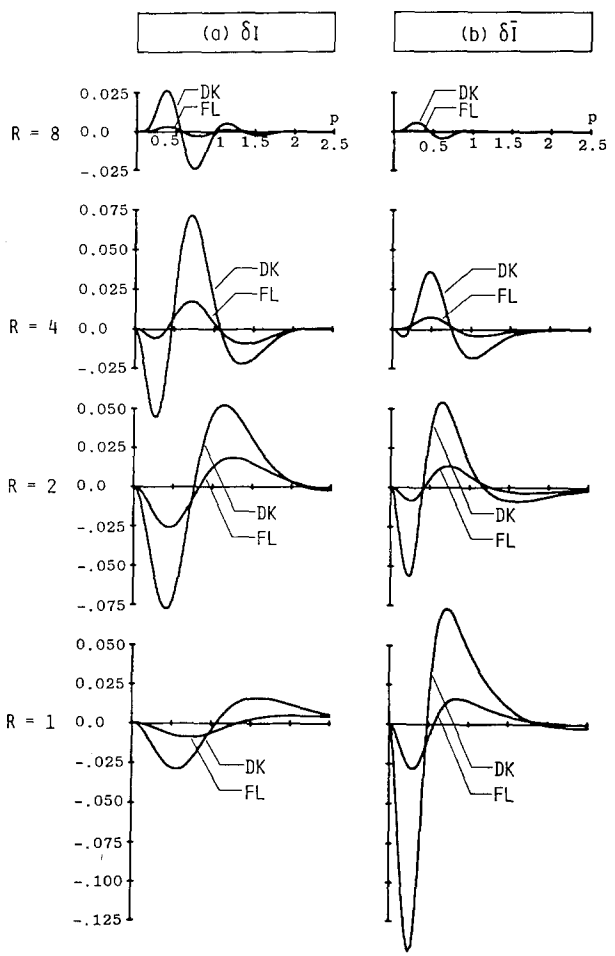

Fig. 3. The polarization and floating effects on the radial momentum densities I and $\bar{I}$

distributions. As discussed in Sect. 3, the DK and FL densities are more expansive than the FH density, reflecting the increased localization of the position density inside the bond. The improvements by the polarization and floating functions are clear and the Duncanson's conclusion [18] that the $I(p)$s for DK and FH are almost superimposable is erroneous. Table 1 compares three nodal points of the p-space wave functions for the molecule along the p_z axis. The results of Fig. 2 and Table 1 show that the improvement is parallel to the accuracy of dissociation energy D_e. However, the third nodal point of FL takes more wrong value than that of FH, and the FL function is seen to "deteriorate" the momentum distribution in high p region. This is attributed to the fact that the floating destroys the density cusps at the nuclei in r-space [10]. Note that though the DK and exact functions have non-periodic nodal points, the FL and FH functions have periodic ones due to the term cos $(Rp_z/2)$.

In Fig. 3a, the density difference δI $[\equiv I - I_{\mathrm{FH}}]$ is given which refers to the polarization and floating effects on the momentum density. (Note that δ indicates changes from FH, while Δ indicates changes from the separated atoms.) At $R = 8$, DK and FL show an increase of low momentum density with an r-space picture of the inward polarization of the atomic density. At this R, the contraction increases and results in $\Delta T_{\mathrm{DK}} < \Delta T_{\mathrm{FL}} < \Delta T_{\mathrm{FH}}$ (Fig. 4c). At $R = 4$, the DK and FL functions have both the contractive and expansive characters when compared with the FH function, suggesting the co-existence of two opposite pictures in r-space, the enlargement of the space of electronic motion due to the accumulation of bond density and the reduction of that space due to the expence of the

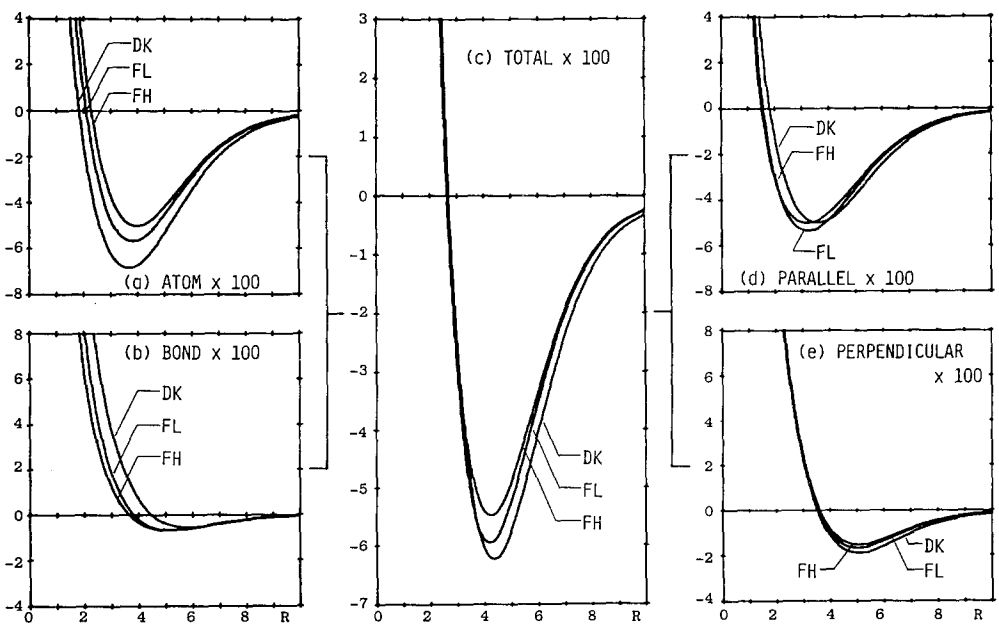

Fig. 4. Kinetic energies obtained from the FH, FL, and DK momentum densities. Their decompositions into the atom–bond and parallel–perpendicular components are also shown

density outside the bond. Because of the expansive $2p\sigma$ AO, the density decrease around $p \sim 0.3$ shows noticeable difference between DK and FL. In r-space, the FL and FH functions with the spherically-symmetric atomic densities do not have sufficient density localization along the bond axis. When the kinetic operator $p^2/2$ is applied, the contractive character dominates over the expansive one and results in $\Delta T_{DK} < \Delta T_{FL} < \Delta T_{FH}$. At $R = 2$, there is an expansive migration with $\Delta T_{DK} > \Delta T_{FL} > \Delta T_{FH}$, corresponding to the r-space deficiency of the density localization in the FH approximation. Since the parameters c_2 and x, which measure the magnitudes of the polarization and floating effects, are nearly maximum at $R = 2$, the reorganizations δI are also maximum at this R. The δIs for $R = 1$ are similar to but smaller than those for $R = 2$. This may reflect the fact that all the three functions converge correctly to the $1s(He^+)$ AO in the united atom limit. In accord with the qualitative discussion in Sect. 3, the polarization and floating functions are indeed found to contribute to increase the contraction and expansion respectively at a large and a small R. Throughout the whole range of R, the polarization effect is larger than the floating effect, and the importance of the directional distortion of the density is suggested in describing the chemical bond.

The redistribution $\delta\bar{I}$ $[\equiv \bar{I} - \bar{I}_{FH}]$ is shown in Fig. 3b, which governs changes in the stabilization energy ΔE (Fig. 5). For $R = 8$ and 4, the two effects promote the contraction of $\bar{I}$ and result in $\Delta E_{DK} < \Delta E_{FL} < \Delta E_{FH}$ in this R range. At $R = 2$, $\delta\bar{I}$ reveals both the expansive and contractive density migrations, but the latter plays a primary role ($\Delta E_{DK} < \Delta E_{FL} < \Delta E_{FH}$) when $p^2/2$ is considered.

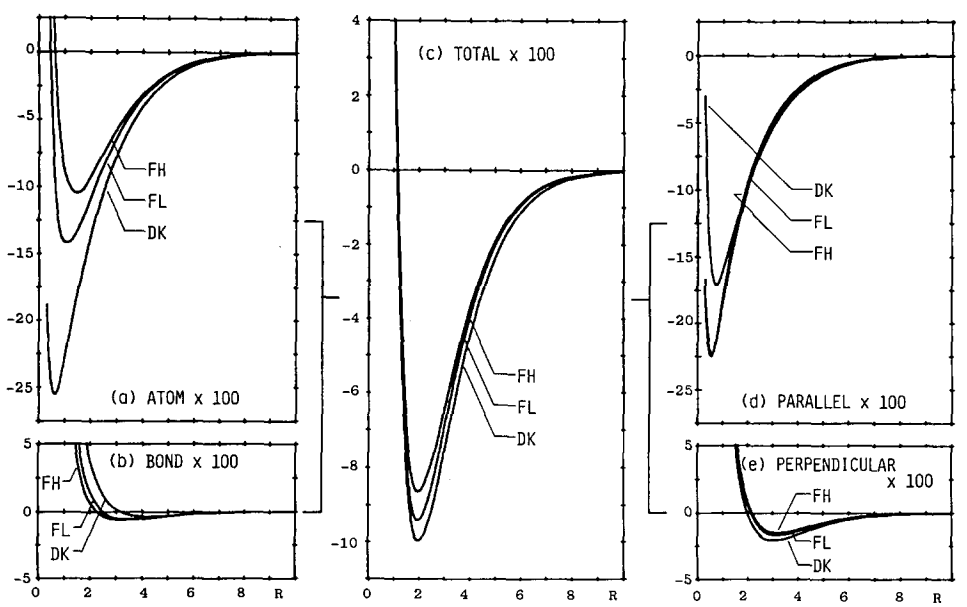

Fig. 5. Stabilization energies obtained from the FH, FL, and DK momentum densities. Their decompositions into the atom–bond and parallel–perpendicular components are also shown

At $R=1$, a pattern of expansion with the density migration from $p\sim 0.3$ to $p\sim 0.7$ is dominant. However, a small density decrease is also observed for $p>1.9$, and then the energy factor $p^2/2$ offsets the effects of these reorganizations, leading to a small energetic change. Since $\delta\bar{I}$ is the integration of δI with the prefactor $1/R$, $\delta\bar{I}$ shows a larger reorganization for a smaller R. Though the $\delta\bar{I}$ connects the density behaviour directly with the stabilization energy, $\delta\bar{I}$ for a small R has little intuitiveness of the proposed guiding principle of contraction and expansion.

Fig. 6 shows the atom–bond partitioning of δI and $\delta\bar{I}$ at $R=4$ and 2. It is seen in Fig. 6a that the reorganization in δI consists of the decrease of low momentum density in the atom part and the increase of high momentum density in the bond part. The contributions of these partitioned densities to the kinetic energy ΔT are given in Figs. 4a and b. Though the bond density suffers primary influence of the polarization and floating functions (see Sect. 3), the change in ΔT_{bond} is

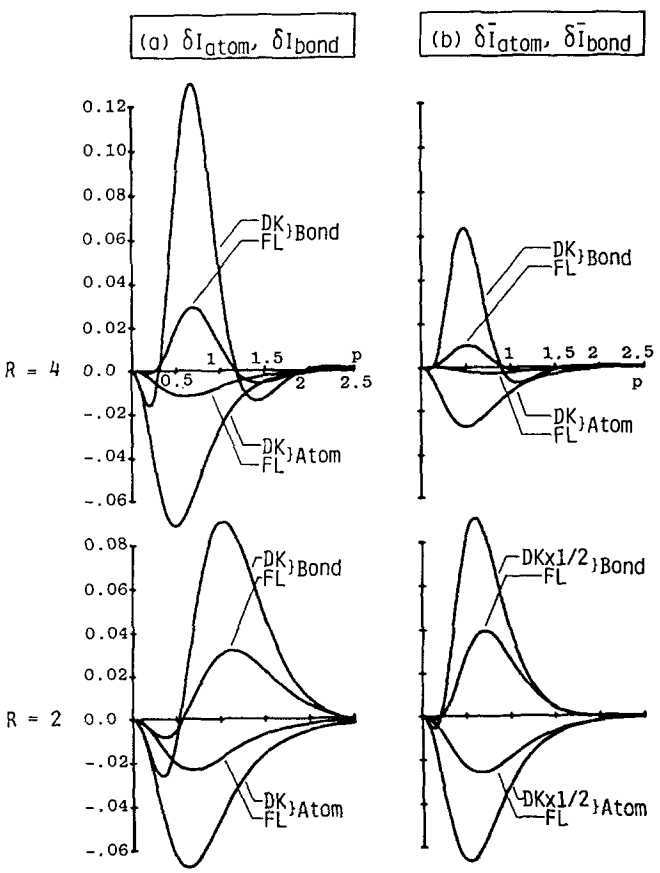

Fig. 6. Atom–bond partitioning of the polarization and floating effects on the momentum density distributions

smaller than that in ΔT_{atom} for $R > 3$. In the atom part, the density decrease reduces the kinetic pressure in this portion and hence lowers ΔT_{atom}, while in the bond part, the decrease in the kinetic pressure due to the density delocalization is nearly counterbalanced with the increase in the kinetic pressure due to the density increase, and ΔT_{bond} remains almost unchanged. For $R < 3$, however, ΔT_{bond} for DK and FL increase considerably, since the localization of the bond density works to raise the kinetic pressure in cooperation with the density increase. Similar behaviours are observed for the atom–bond partitionings of $\delta \bar{I}$ (Fig. 6b) and ΔE (Figs. 5a and b). As a result, the polarization and floating effects on the atom–bond partitioning emphasize the importance of the atom and bond parts respectively in the initial and final stages of the bond formation.

Fig. 7 shows the reorganizations in the directional Compton profiles. The parallel part $\delta J_{\parallel}$ at $R = 4$ (Fig. 7a) shows both of the contraction and expansion, reflecting the fact that the increased overlap in DK and FL not only decreases the kinetic pressure in the internuclear region (contractive effect) but also reduces the effective length of electron motion in the parallel direction (expansive effect).

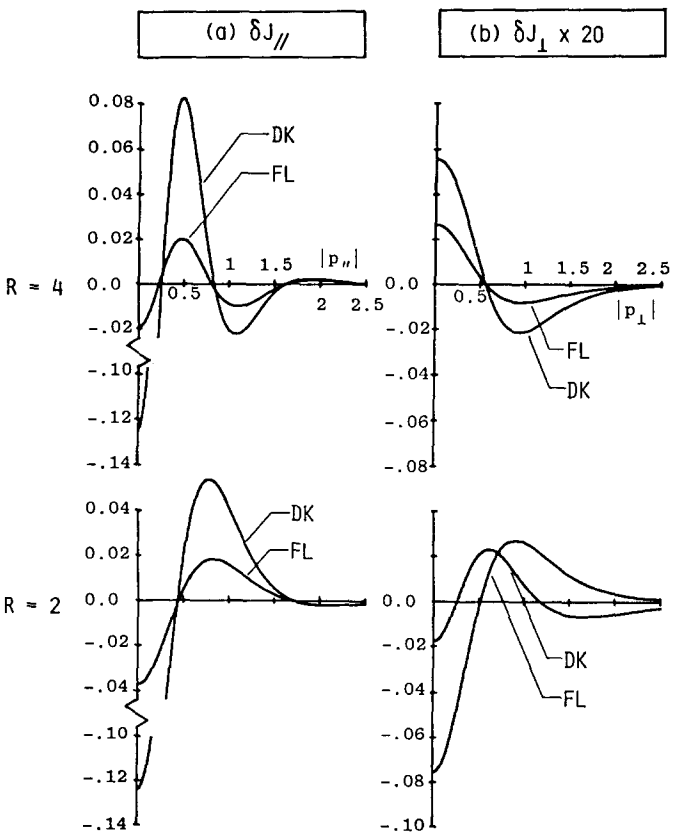

Fig. 7. The polarization and floating effects on the directional Compton profiles

Energetically, the former gives larger contribution and $\Delta T_{\parallel}$ lowers for DK and FL (Fig. 4d). However, the expansive effect dominates at a smaller R (e.g. $R = 2$), leading to an increase of $\Delta T_{\parallel}$. The changes in the perpendicular part $\delta J_{\perp}$ (Fig. 7b) are very small as expected in the previous section. At $R = 4$, $\delta J_{\perp}$ is contractive and $\Delta T_{\perp}$ lowers (Fig. 4e) due to the mixing of the $2p\sigma$ AO which is more contractive than the $1s$ AO in this direction (DK) and due to the decrease of the orbital exponent (FL). At $R = 2$, the expansive change and the increase in $\Delta T_{\perp}$ appear, since the position density becomes bound more tightly to the nuclei (an increase in orbital exponent) with the concomitant increase in the kinetic pressure. Except for a very small R, the polarization and floating effects on the partitioned energies are smaller for the directional partitioning than for the atom–bond one (Figs. 4 and 5). This may suggest the basis-dependence of the latter partitioning in this approach.

5. Summary

Based on the recently proposed method of momentum density, the pictures and roles of the the polarization and floating functions in p-space have been studied. Referring to the momentum density of the minimal LCAO FH function, we have quantitatively examined the density redistributions due to the DK and FL functions together with their energetic contributions for the prototype bonding process in the H_2^+ system. The essential points of the polarization and floating effects have been shown to be the modulation of the two-center part of momentum density by the addition of a term with a phase (DK) and by the enlargement of the period of oscillation (FL). The increased density migration from the one-center to the two-center part is also important. As a result, the low momentum density increases at a large R, whereas the high momentum density increases at a small R. The former reflects the increased delocalization of the atomic density, while the latter suggests that the density accumulation in the bond region has a picture of localization at a small R. These density reorganizations are larger for DK than for FL throughout the bonding process. The improvement by the FL function is shown to include the disturbance of high momentum distribution, corresponding to the destruction of cusps in r-space. The polarization and floating functions work to emphasize the contraction and expansion of momentum density during the process, and the reliability of the previous discussion [2] based on the FH density has been confirmed.

Acknowledgment. Part of this study has been supported by a Grant-in-Aid for Scientific Research from the Ministry of Education of Japan.

References

1. Koga, T.: Theoret. Chim. Acta (Berl.) **58**, 173 (1981)
2. Koga, T., Morita, M.: Theoret. Chim. Acta (Berl.) **59**, 423 (1981)
3. Koga, T., Morita, M.: Theoret. Chim. Acta (Berl.) **59**, 639 (1981)

4. Koga, T., Sugawara, M., Morita, M.: Theoret. Chim. Acta (Berl.) **61**, 87 (1982)
5. Koga, T., Morita, M.: Theoret. Chim. Acta (Berl.) **61**, 73 (1982)
6. Finkelstein, B. N., Horowitz, G. E.: Z. Phys. **48**, 118 (1928)
7. Epstein, S. T., Hurley, A. C., Wyatt, R. E., Parr, R. G.: J. Chem. Phys. **47**, 1275 (1967)
8. Steiner, E.: The determination and interpretation of molecular wave functions. London: Cambridge U.P. 1976
9. Miller, R. L., Lykos, P. G.: J. Chem. Phys. **35**, 1147 (1961); **37**, 993 (1962); Geller, M., Frost, A. A., Lykos, P. G.: J. Chem. Phys. **36**, 2693 (1962)
10. Pilar, F. L.: Elementary quantum chemistry. New York: McGraw-Hill 1968
11. Hurley, A. C.: Proc. Roy. Soc. London **A226**, 179 (1954); Introduction to the electron theory of small molecules. New York: Academic 1976
12. Shull, H., Ebbing, D. D.: J. Chem. Phys. **28**, 866 (1958)
13. Hellmann, H.: Einführung in die Quantenchemie. Vienna: Deuticke 1937; Feynman, R. P.: Phys. Rev. **56**, 340 (1939)
14. Deb, B. M., ed.: The force concept in chemistry. New York: Van Nostrand Reinhold 1981
15. Dickinson, B. N.: J. Chem. Phys. **1**, 317 (1933); Weinhold, F.: J. Chem. Phys. **50**, 530 (1971)
16. Dirac, P. A. M.: The principles of quantum mechanics. London: Oxford U.P. 1958
17. Abramowitz, M., Stegun, I. A. ed.: Handbook of mathematical functions. New York: Dover 1970
18. Duncanson, W. E.: Proc. Camb. Phil. Soc. **37**, 397 (1941)
19. Thomas, M. W.: Mol. Phys. **23**, 571 (1972)
20. Liu, J. W., Smith, Jr., V. H.: Mol. Phys. **35**, 145 (1978)
21. Glaser, F. M., Lassettre, E. N.: J. Chem. Phys. **44**, 3787 (1966)
22. Bates, D. R., Ledsham, K., Stewart, A. L.: Phil. Trans. Roy. Soc. London **A246**, 215 (1954)

Received May 11, 1982